

Chiral heat transport in driven quantum Hall and quantum spin Hall edge statesLiliana Arrachea¹ and Eduardo Fradkin²¹*Departamento de Física, Facultad de Ciencias Exactas y Naturales, Universidad de Buenos Aires, Pabellón 1, Ciudad Universitaria, 1428, Buenos Aires, Argentina*²*Department of Physics, University of Illinois at Urbana-Champaign, 1110 West Green Street, Urbana, Illinois 61801-3080, USA*
(Received 3 October 2011; revised manuscript received 4 December 2011; published 21 December 2011)

We consider a model for an edge state of electronic systems in the quantum Hall regime with filling $\nu = 1$ and in the quantum spin Hall regime. In both cases, the system is in contact with two reservoirs by tunneling at point contacts. Both systems are locally driven by applying an ac voltage in one of the contacts. By weakly coupling them to a third reservoir, the transport of the generated heat is studied in two different ways: (i) when the third reservoir acts as a thermometer, the local temperature is sensed and (ii) when the third reservoir acts as a voltage probe, the time-dependent local voltage is sensed. Our results indicate a chiral propagation of the heat along the edge in the quantum Hall and in the quantum spin Hall cases (if the injected electrons are spin polarized). We also show that an analogous picture is obtained if instead of heating by ac driving the system is put in contact to a stationary reservoir at a higher temperature. In both cases, the temperature profile shows that the electrons along the edge thermalize with the closest “upstream” reservoir.

DOI: [10.1103/PhysRevB.84.235436](https://doi.org/10.1103/PhysRevB.84.235436)

PACS number(s): 73.43.Jn, 72.10.Bg, 72.80.Vp, 73.23.Ad

I. INTRODUCTION

A key and almost defining property of quantum Hall states, integer¹ and fractional,² is the existence of a structure of gapless states at the boundary of these incompressible quantum fluids, which propagate only along a direction dictated by the external perpendicular magnetic field, chiral edge states. The experimental detection of the chiral nature of these states is thus crucial to the understanding of these fluids and has been the focus of intense research, in experiment and theory alike.³ The recently discovered two-dimensional topological insulators, strong spin-orbit coupled semiconductors that exhibit a quantized anomalous Hall effect (if spin polarized) or the quantum spin Hall effect (if unpolarized), are also predicted to have a universal edge structure.⁴ In the anomalous quantum Hall state, the edge states are chiral whereas in the quantum spin Hall effect the edge states with opposite polarization propagate in opposite directions.

In a recent very interesting experiment, evidence of chiral propagation of the heat along an edge state in a GaAs/AlAs heterostructure with a two-dimensional electron gas in the integer quantum Hall regime has been presented.⁵ The experiment was performed in the quantum Hall regime with filling $\nu = 1$ locally heated by an ac field. Heat transport in ac driven systems have been recently the focus of experimental and theoretical interest in several electronic,^{6–9} phononic,¹⁰ and photonic¹¹ systems. So far experiments of this type have not been done in graphene-based devices, which have the advantage that the integer quantum Hall effect is seen at room temperature¹² or in two-dimensional topological insulators. The goal of the present work is the theoretical analysis of a setup close to the experimental work for the integer quantum Hall case.⁵ Our model and results should also apply to graphene, and we also generalize it to quantum spin Hall systems. As we will see below, our results verify the empirical conclusions of Ref. 5 regarding the chiral propagation of the heat along the edge. Another conclusion of that work is the electronic cooling in the propagation along the edge. Our results indicate that the propagation is coherent along the edge,

the electrons preserving some “memory” of the temperature of the last reservoir they have visited.

We base our study in a microscopic model for the edge, consistent in a ring of free chiral fermions connected to two fermionic reservoirs through tunneling couplings, as indicated in the sketch of Fig. 1. In the case of the spin Hall case, sketched in Fig. 1(b), we consider two states in the edge, corresponding to electrons moving with opposite chirality and helicity. We also consider the possibility of spin-polarized reservoirs in the latter case. In one of the reservoirs, an ac voltage is applied, acting as a local heater. We consider a weak coupling to a third reservoir, which will be used to define a voltage probe or a thermometer. Both kinds of probes are used to sense the local temperature along the edge. In the case of the voltage probe, the signal of the time-dependent voltage is experimentally used to get an estimate of the local temperature from thermoelectric effects.^{5,13} A thermometer is defined in a gedanken setup, where the temperature of a weakly coupled reservoir is fixed from the condition of a vanishing heat flow through the contact to the system under investigation. That definition of temperature was originally proposed in Ref. 14 in the context of stationary electronic transport. It has been adopted to analyze stationary transport¹⁵ in nanodevices and generalized to the context of systems under ac driving.⁹ This definition of the local temperature is correct if the system is weakly driven, and agrees with other definitions of the temperature from fluctuation-dissipation relations in nonequilibrium systems.^{8,9,16}

This work is organized as follows. In Sec. II, we present a simple model that mimics the setup of Granger *et al.*⁵ and we generalize it for the case of spin-Hall effect. In Sec. III, we derive expressions for the heat current in terms of Green functions of chiral fermions in this nonequilibrium situation. In Secs. IV and V, we present a theory of sensing with voltage probes and thermometers along the edge, respectively. In Sec. VI, we present results for the heat propagation in the cases of the quantum Hall as well as in the quantum spin Hall effect. Section VII is devoted to the conclusions.

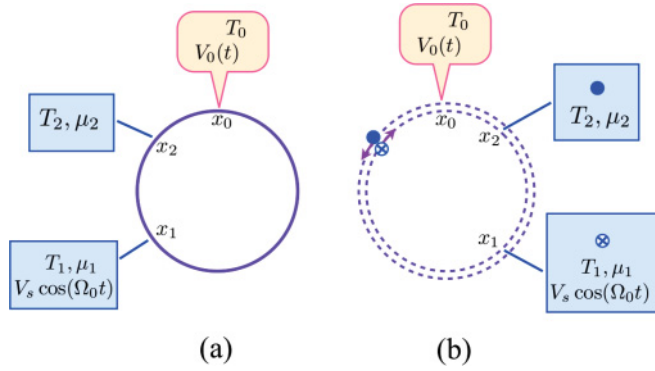


FIG. 1. (Color online) Sketch of the considered setup. (a) The quantum Hall edge state is represented by a circle. Two reservoirs are connected at the positions x_1 (source) and x_2 (drain). An ac voltage is applied at the source reservoir. A third reservoir is weakly connected at x_0 in order to sense the local voltage $V_0(t)$ or the local temperature T_0 . (b) Quantum spin Hall effect. The system contains a pair of edge states where electrons with spin up (down) move clockwise (counterclockwise). The source and drain reservoirs are spin polarized.

II. MODEL

The full system is described by the following Hamiltonian:

$$H = H_{\text{edge}} + \sum_{j=0}^2 [H_j + H_{c,j}] + H_{\text{ac}}(t), \quad (1)$$

where the edge is represented by a ring of circumference L along which chiral fermions circulate with velocity v_F . In the case of topological insulators (the spin quantum Hall state), there are two edge states (Kramers pairs) with opposite chiralities and helicities (which we will refer to as “spin”). The Hamiltonian for the edge states in the latter case is

$$\begin{aligned} H_{\text{edge}} &= \sum_{\sigma=\pm} \int_0^L dx \Psi_{\sigma}^{\dagger}(x) \mathcal{D}_x \partial_x \Psi_{\sigma}(x) \\ &= \sum_{p,\sigma} v_{F,\sigma} \left(p - \frac{\Phi}{L} \right) \Psi_{p,\sigma}^{\dagger} \Psi_{p,\sigma}, \end{aligned} \quad (2)$$

where $\mathcal{D}_x = -i v_{F,\sigma} \partial_x - \Phi/L$, with Φ the magnetic flux threading the ring in units of the flux quantum eh/c . We assume that the electrons moving clockwise have spin \uparrow , while those moving counterclockwise have spin \downarrow . Thus $v_{F,\sigma} = \sigma v_F$ with $p = 2n\pi/L$, where n is an integer and $|p| \leq K$, while

$$H_j = -i \sum_{\sigma=\pm} v_{F,\sigma}^j \int_0^{\infty} dr_j \Psi_{\sigma}^{\dagger}(r_j) \partial_{r_j} \Psi_{\sigma}(r_j), \quad (3)$$

are the Hamiltonians of infinite systems of chiral fermions, which play the role of reservoirs. The source ($j = 1$) and drain ($j = 2$) reservoirs are at temperatures T_1 and T_2 , respectively, and have the same chemical potential μ . We consider the possibility for the reservoirs $j = 1, 2$ to be spin polarized, which is equivalent to assuming $v_{F,+}^j \neq v_{F,-}^j$, $j = 1, 2$. The system is driven by applying an ac voltage $V_1(t) = V_s \cos(\Omega_0 t)$ at the reservoir $j = 1$. The reservoir $j = 0$ corresponds to a probe that may act as a thermometer or a voltage probe. In the first case, it has the same chemical potential μ as the other

reservoirs, while its temperature T_0 is adjusted in order to satisfy the condition of vanishing heat flow along its contact to the ring. In the second case, it has the same temperature as the other reservoirs, while it has an ac voltage $V_0(t) = \mu_0 + \sum_{k \neq 0} e^{-i(k\Omega_0 t + \varphi_k)} V_0^{(k)}/2$. The different harmonics $V_0^{(k)}$ are adjusted to satisfy the condition of a vanishing charge flow along the contact.

The time-dependent voltages can be described in terms of the Hamiltonian

$$H_{\text{ac}}(t) = \sum_{j=0,1,\sigma} V_j(t) \int \frac{dp_j}{2\pi} \Psi_{p_j,\sigma}^{\dagger} \Psi_{p_j,\sigma}. \quad (4)$$

The contacts are described by the Hamiltonians

$$H_{c,j} = w_j \sum_{\sigma} [\Psi_{\sigma}^{\dagger}(x_j) \Psi_{\sigma}(r_j^0) + \text{H.c.}], \quad (5)$$

where x_j and r_j^0 are the positions of the ring and the reservoir, respectively, at which the contact is established. We assume that the tunneling parameter w_0 between the ring and the probe reservoir is so weak that it introduces negligible dephasing in the particle propagation along the ring.

In the case of the usual quantum Hall effect, there is just one edge state and the spin label becomes irrelevant. Thus, in order to model that case, we should consider the above Hamiltonian with just one of the helicities σ .

In the following sections, we will compute the local temperature by sensing with a thermometer, and voltage by sensing with a voltage probe, along the edges for each of these systems.

III. CHARGE AND HEAT CURRENTS THROUGH THE CONTACT TO THE PROBE

The expression for the charge and heat currents flowing through the contact between the edge and the probe reservoir are obtained from the general laws of the conservation of the charge and energy, respectively,

$$\begin{aligned} \frac{d\langle N_0 \rangle}{dt} &= J_0^c(t) = 2w_0 \sum_{p_0,\sigma} \text{Re}[e^{-ip_0 r_0^0} G_{x_0,p_0,\sigma}^<(t,t)], \\ \frac{d\langle H_0 - \mu N_0 \rangle}{dt} &= J_0^Q(t) \\ &= 2w_0 \sum_{p_0,\sigma} \text{Re}[e^{-ip_0 r_0^0} (\varepsilon_{p_0,\sigma} - \mu) G_{x_0,p_0,\sigma}^<(t,t)], \end{aligned}$$

where $N_0 = \sum_{p_0,\sigma} \Psi_{p_0,\sigma}^{\dagger} \Psi_{p_0,\sigma}$, $\varepsilon_{p_0,\sigma} = \sigma v_F^0 p_0$, while we have introduced the lesser Green function $G_{x_0,p_0,\sigma}^<(t,t') = i \langle \Psi_{p_0,\sigma}^{\dagger}(t') \Psi_{\sigma}(x_0,t) \rangle$. Since both currents are generated by an ac voltage of frequency Ω_0 they can be in general expressed as

$$J_0^{c,Q}(t) = \sum_k e^{-ik\Omega_0 t} J_0^{c,Q}(k). \quad (6)$$

The lesser Green function satisfies the following Dyson equation

$$\begin{aligned} G_{x_0,p_0,\sigma}^<(t,t') &= w_0 \int_{-\infty}^{+\infty} dt_1 [G_{x_0,x_0,\sigma}^<(t,t_1) g_{k_0,\sigma}^A(t_1,t') \\ &\quad + G_{x_0,x_0,\sigma}^R(t,t_1) g_{p_0,\sigma}^<(t_1,t')], \end{aligned} \quad (7)$$

where we have introduced the retarded Green function $G_{x,x',\sigma}^R(t,t') = -i\Theta(t-t')\langle\{\Psi_\sigma(x,t),\Psi_\sigma^\dagger(x',t')\}\rangle$ as well as

$$g_{p_0,\sigma}^{R(<)}(t,t') = g_{p_0,\sigma}^{R(0,<)}(t-t')\phi_0(t,t'), \quad (8)$$

where

$$\begin{aligned} g_{p_0,\sigma}^A(t,t') &= [g_{p_0,\sigma}^R(t',t)]^*, \\ g_{p_0,\sigma}^{0,R}(t-t') &= -i\Theta(t-t')\exp[-i\varepsilon_{p_0,\sigma}(t-t')], \\ g_{p_0,\sigma}^{0,<}(t-t') &= i2\pi f(\varepsilon_{p_0,\sigma} - \mu_0)\exp[-i\varepsilon_{p_0,\sigma}(t-t')]. \end{aligned} \quad (9)$$

Here, $f(\varepsilon_{p_0,\sigma} - \mu_0)$ is the Fermi function with a chemical potential μ_0 and temperature T_0 . The function $\phi_0(t,t')$ contains information on the ac-potentials applied at the probe

$$\begin{aligned} \phi_0(t,t') &= \exp\left[-i\sum_{k=1}^2 V_0^{(k)} \int_{t'}^t dt_1 \cos(k\Omega_0 t_1 + \varphi_k)\right] \\ &\simeq 1 - i\sum_{k=1}^2 V_0^{(k)} \int_{t'}^t dt_1 \cos(k\Omega_0 t_1 + \varphi_k) + \dots, \end{aligned} \quad (10)$$

where in the second line, we have assumed that the amplitudes $V_0^{(k)}$ are low enough. For the probe acting as a thermometer, $V_0^{(k)} = 0$ and $\mu_0 = \mu_1 = \mu_2 \equiv \mu$. Thus $\phi_0(t,t') = 1$, while T_0 defines the sensed local temperature, which is determined from the condition $J_0^Q(0) = 0$.⁹ For the probe acting as a voltage probe, we consider $T_0 = T_1 = T_2 \equiv T$, while $\mu_0, V_0^{(k)}$, and φ_k are determined by demanding the conditions $J_0^c(k) = 0$, $k = -2, \dots, 2$.¹⁷

Following the procedure of Ref. 18, it is convenient to take explicitly into account the harmonic time dependence of

$$\begin{aligned} J_0^c(t) &= 2\text{Re}\left\{\sum_{k,\sigma} e^{-ik\Omega_0 t} \int \frac{d\omega}{2\pi} [\mathcal{G}_{x_0,x_0,\sigma}^{<}(k,\omega)\Sigma_0^A(\omega) + \mathcal{G}_{x_0,x_0,\sigma}(k,\omega)\Sigma_0^{<}(\omega)] + \sum_{s=\pm 1} \sum_{n=1}^2 s \frac{V_0^{(n)}}{2\Omega_0} e^{-is\varphi_n}\right. \\ &\quad \left.\times \{[\mathcal{G}_{x_0,x_0,\sigma}^{<}(k-sn,\omega_{sn}) - \mathcal{G}_{x_0,x_0,\sigma}^{<}(k-sn,\omega)]\Sigma_0^A(\omega) + [\mathcal{G}_{x_0,x_0,\sigma}(k-sn,\omega_{sn}) - \mathcal{G}_{x_0,x_0,\sigma}(k-sn,\omega)]\Sigma_0^{<}(\omega)\}\right\}, \end{aligned} \quad (14)$$

where

$$\begin{aligned} \Sigma_0^A(\omega) &= w_0^2 \sum_{k_0} [g_{k_0}^0(\omega)]^* \sim i\Gamma_0/2, \\ \Sigma_0^{<}(\omega) &= if_0(\omega)w_0^2 \sum_{k_0} \delta(\omega - \varepsilon_{k_0}) \sim if_0(\omega)\Gamma_0, \end{aligned} \quad (15)$$

with $f_0(\omega) = f(\omega - V_0)$ and $\Gamma_{0,\pm} = \Gamma_0$.

Since we consider a weak coupling w_0 , we shall neglect terms $\propto w_0$ in the evaluation of the functions $\mathcal{G}_{x_0,x_0,\sigma}(k,\omega)$ and $\mathcal{G}_{x_0,x_0,\sigma}^{<}(k,\omega)$. This corresponds to evaluating these Green functions considering just the coupling to the source reservoir and neglecting the coupling to the probe and the resulting current $J_0^c(t)$ is exact up to $\mathcal{O}(w_0^2)$. For the source reservoir, we can define $\Sigma_{j,\sigma}^A(\omega) \sim i\Gamma_{j,\sigma}/2$, $j = 1, 2$, and

the problem, considering the following representation for the Green functions:

$$G_{x,x',\sigma}^{R,<}(t,t') = \sum_k e^{-ik\Omega_0 t} \int \frac{d\omega}{2\pi} \mathcal{G}_{x,x',\sigma}^{R,<}(k,\omega) e^{-i\omega(t-t')}. \quad (11)$$

In the evaluation of the Green functions for coordinates within the ring, it is also convenient to integrate out the degrees of freedom of the reservoirs by defining the following ‘‘self-energies’’:

$$\Sigma_{j,\sigma}^{R,<}(t,t') = i\phi_j(t,t') \int \frac{d\omega}{2\pi} \lambda_j^{R,<}(t-t',\omega) \Gamma_{j,\sigma}(\omega) e^{-i\omega(t-t')}, \quad (12)$$

where $\lambda_j^R(t-t',\omega) = -i\Theta(t-t')$ and $\lambda_j^{<}(t-t',\omega) = if_j(\omega)\Theta(t-t')$ with $f_j(\omega)$ the Fermi function, which depends on the temperature and the chemical potential of the reservoir while the functions $\phi_j(t,t')$ take into account the applied ac voltages. For our configuration, $\phi_2(t,t') = 1$, while

$$\begin{aligned} \phi_1(t,t') &= \exp\left\{-iV_S \int_{t'}^t dt_1 \cos(\Omega_0 t_1)\right\} \sim 1 - iV_S \\ &\quad \times \int_{t'}^t dt_1 \cos(\Omega_0 t_1) - \frac{V_S^2}{2} \left[\int_{t'}^t dt_1 \cos(\Omega_0 t_1)\right]^2, \end{aligned} \quad (13)$$

where we have assumed in the second step that the amplitude V_S is small.

IV. SENSING WITH A VOLTAGE PROBE

Substituting Eq. (7) and the representation Eq. (11) in the expression of Eq. (6) for the charge current results in

$\Sigma_{j,\sigma}^{<}(\omega) = if_j(\omega)\Gamma_{j,\sigma}$, where $f_j(\omega) = 1/[1 + e^{\beta_j(\omega-\mu)}]$, with $\beta_j = T_j^{-1}$, $j = 1, 2$.

After some algebra, for low driving frequency Ω_0 ,²⁰ the solution of the set of conditions $J_0^c(k) = 0$, $k = -2, \dots, 2$ yields the results for the chemical potential and voltage profiles [to order $\mathcal{O}(V_S^2)$]:

$$\begin{aligned} \mu_0 &= \mu - \left(\frac{V_S}{2}\right)^2 \frac{\alpha'(\mu)}{\rho_{x_0}(\mu)}, \\ V_0^{(1)} &= V_S \frac{\alpha(\mu)}{\rho_{x_0}(\mu)}, \\ V_0^{(2)} &= \frac{1}{2} \left(\frac{V_S}{2}\right)^2 \frac{\alpha'(\mu)}{\rho_{x_0}(\mu)}, \end{aligned} \quad (16)$$

where $\rho_{x_0}(\omega) = -2 \sum_{\sigma} \text{Im}[G_{x_0, x_0, \sigma}^0(\omega)]$ and $\alpha(\omega) = \sum_{\sigma} |G_{x_0, x_1, \sigma}^0(\omega)|^2 \Gamma$, where $G_{x, x', \sigma}^0(\omega)$ is the equilibrium retarded Green function of the edge connected to the reservoirs $j = 1, 2$. Notice that the behavior of these three harmonics is not independent one another, since $\mu_0 - \mu = -2V_0^{(2)}$, where these quantities are determined by the value of the function $\alpha(\omega)$ evaluated at μ , while $V_0^{(1)}$ is determined by the derivative of this function.

V. SENSING WITH A THERMOMETER

The dc component of the heat current defined in Sec. III can be written as follows:

$$J_0^Q(0) = \Gamma_0 \int \frac{d\omega}{2\pi} (\omega - \mu) \{ i \mathcal{G}_{x_0, x_0, \sigma}^<(0, \omega) - 2f_0(\omega) \text{Im}[\mathcal{G}_{x_0, x_0, \sigma}(0, \omega)] \}. \quad (17)$$

Calculating the Green functions $\mathcal{G}_{x_0, x_0, \sigma}^<(0, \omega)$, while keeping terms up to $\mathcal{O}(V_S^2)$ and expanding in Ω_0 and T_0 , the condition $J_0^Q(0) = 0$ now leads to the result

$$T_0^2 = \frac{[T_1^2 + 3V_S^2/(2\pi^2)]\alpha'_1(\mu) + T_2^2\alpha'_2(\mu)}{\alpha'_0(\mu)}, \quad (18)$$

where T_j are the temperatures of the reservoirs $j = 1, 2$, respectively, while

$$\begin{aligned} \alpha_0(\omega) &= (\omega - \mu)\rho_{x_0}(\omega), \\ \alpha_j(\omega) &= (\omega - \mu) \sum_{\sigma} |G_{x_0, x_j, \sigma}^0(\omega)|^2 \Gamma_{j, \sigma}, \quad j = 1, 2. \end{aligned} \quad (19)$$

It is interesting to mention that in the limit where $V_S \rightarrow 0$, the temperature T_0 defined in Eq. (18) reduces to the local temperature sensed by a thermometer when the heat transport is induced in purely stationary conditions by connecting the ring to reservoirs with different temperatures $T_1 \neq T_2$. Thus the ac driving renormalizes the temperature of the reservoir at which it is applied by a factor $\propto V_S$. In particular, for reservoirs at equal temperature $T_1 = T_2 = 0$, the effect of the ac driving is equivalent to having the source reservoir at a temperature $T_1 = \sqrt{3/2}V_S/\pi$.

Another interesting feature is the fact that we can approximate the functions $\alpha'_0(\mu) \approx \rho_{x_0}(\mu)$ and $\alpha'_1(\mu) \approx \alpha(\mu)$. For a source reservoir at $T_2 = 0$, we then find

$$T_0 = \frac{T_1}{\sqrt{\rho_{x_0}}} + \frac{3V_S\sqrt{\rho_{x_0}}}{4\pi^2} V_0^{(1)}, \quad (20)$$

which suggests a rather straightforward relation between the local temperature and the first harmonic of the local voltage. This is somehow in contrast with the assumption, done in the experimental work, that the second harmonic is more sensitive to the heat transport than the first one. We will show in the next section, however, that the three harmonics analyzed in the present work contain the relevant signatures of the behavior of the heat propagation along the edge.

Finally, we would like to mention that it is possible to simultaneously define the local voltage as well as the temperature from the conditions $J_0^c(t) = J_0^Q(0) = 0$. It has been, however, shown in Ref. 9 that, within the weak driving regime (small amplitudes and low frequency of the ac potentials), such

definitions coincide with the ones we consider in the present and the preceding sections.

VI. RESULTS

A. Quantum Hall edge

We begin analyzing the usual quantum Hall case, which corresponds to the Hamiltonian of Eq. (1) with a single chirality, which we assume to be $\sigma = +$. The unperturbed retarded Green function $G_{x, x', \sigma}^0(\omega)$ is evaluated in Appendix. The expression for the harmonics of the sensed local voltage, Eq. (16), involves the local density of states $\rho_{x_0}(\omega) = \Theta(\Lambda - |\omega|)\pi/\Lambda$ (where Λ is a high-energy cutoff), and the functions $\alpha(\omega)$ and $\gamma(\omega)$, which in this case are given by

$$\alpha(\omega) = \begin{cases} \gamma(\omega) & \text{if } x < x_1, \quad x \geq x_2, \\ \gamma(\omega)(1 + \bar{\Gamma}_{2,+}) & \text{if } x_1 \leq x < x_2. \end{cases}$$

and

$$\gamma(\omega) = \frac{\pi \bar{\Gamma}_{1,+}}{4\Lambda |\Delta_+(\omega)|^2 \sin^2\left(\frac{\omega L}{2v_F} + \frac{\Phi}{2}\right)}. \quad (21)$$

Thus, for fixed values for the length of the edge L , the Fermi velocity of the electrons along the edge, v_F and the chemical potential μ , the different harmonics of the local voltage have piecewise constant profiles as functions of the position of the voltage probe, the amplitude being a factor $(1 + \bar{\Gamma}_{2,+})$ larger upstream than downstream, while they display discontinuities at the positions x_1 and x_2 at which the source and drain reservoirs are coupled. The same behavior is found for the local temperature (18) sensed by the thermometer. In fact, assuming $T_2 = 0$, $\alpha'_1(\omega) \sim \alpha(\omega)$ and $\alpha'_0(\omega) = \rho_{x_0}(\omega)$. Thus the local temperature is a factor $\sqrt{1 + \bar{\Gamma}_{2,+}}$ higher upstream than downstream. Typical profiles are shown in Fig. 2. In the case of considering a finite cutoff in the energy spectrum of the edge, the three harmonics of the local voltage as well as the local temperature display oscillations as functions of x_0 , which are mounted in the stepwise profile. The frequency and amplitude of these oscillations go to zero in the limit of infinite cutoff considered in Fig. 2. The behavior observed in this figure is exactly the opposite when the movements of the electrons is inverted. This behavior is consistent with electrons heated by the ac voltage and the ensuing current injected through the contact to the source reservoir. The heated electrons propagate chirally until they reach the drain electrode, where they tend to thermalize to the temperature of this reservoir, by means of inelastic scattering processes, with particles and energy exchanged at the corresponding contact. The net flow into the edge keeps propagating chirally at an effective temperature that is close to the one of the drain reservoir until they reach again the source reservoir.

We also notice that the local voltage and temperature display a nontrivial behavior as functions of the magnetic field B . The magnetic field enters in the function $|\Delta_+(\omega)|^2 \sin^2\left(\frac{\omega L}{2v_F} + \frac{\Phi}{2}\right)$ of the denominator of $\gamma(\omega)$, through the magnetic flux Φ as well in the field-dependence of the Fermi velocity, $v_F = \mathcal{E}/\Phi$, with $\mathcal{E} = EL^2c/(4\pi eh)$, being E the electric field. In Fig. 3, we show the different harmonics of the time-dependent local voltage as well as the local temperature as functions of B . We consider fixed μ , L , and positions x_1 and x_2 for the

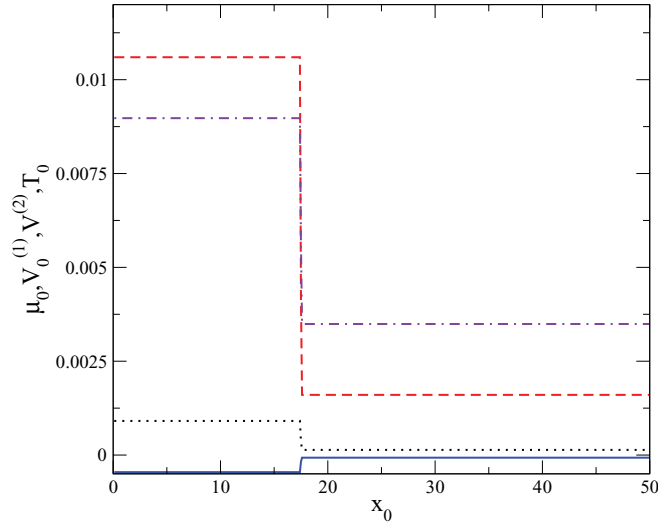


FIG. 2. (Color online) Sensed harmonics of the local time-dependent potential $\mu_0 - \mu$ (dotted line), $V_0^{(1)}$ (dashed line), and $V_0^{(2)}$ (solid line), and local temperature T_0 (dashed-dotted line) as functions of the position of the voltage probe x_0 along a ring of $L = 50$ with electrons moving clockwise with Fermi velocity $v_F = 1$. The source and drain reservoirs are connected at $x_1 = 0$ and $x_2 = 0.35L$, respectively. The chemical potential is $\mu = 0.05$, the coupling parameters are $\bar{\Gamma}_{1,+} = \bar{\Gamma}_{2,+} = \pi$, the temperatures of the reservoirs are $T_1 = T_2 = 0$ and the amplitude of the ac voltage applied at the source is $V_S = 0.05$.

source and drain connections. The upper panel corresponds to sensing at a position $x_1 < x_0 < x_2$ (upstream), while the lower panel corresponds to a downstream position of the probes. The behavior of the harmonics $V_0^{(1)}$ and $V_0^{(2)}$ of the local voltage qualitatively resembles that observed in Fig. 3 of the

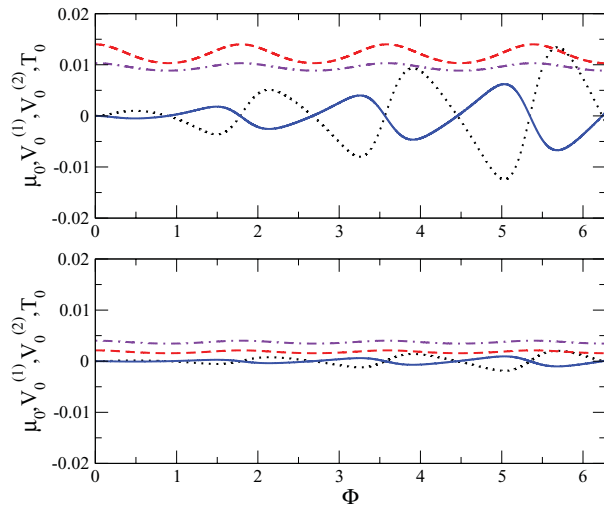


FIG. 3. (Color online) Sensed dc component of the local voltage $\mu_0 - \mu$ (dotted line), first harmonic $V_0^{(1)}$ (dashed line), second harmonic $V_0^{(2)}$ (solid line), and local temperature T_0 (dashed-dotted line) as functions of the applied magnetic flux Φ for $\mathcal{E} = 1$. The remaining parameters are the same as in Fig. 2. The upper panel corresponds to sensing upstream ($x_1 < x_0 < x_2$), while the lower panel corresponds to sensing downstream ($x_0 > x_2$).

experimental work.⁵ Our results show that the ‘‘amplification factor’’ in the upstream signals relative to the downstream ones is fully determined by the degree of coupling of the drain reservoir, represented by $\bar{\Gamma}_{2,+}$. As stressed in the previous section, such amplification, which is the signature of the chiral propagation of the charge and heat currents along the edge, are observed in all the harmonics of the local voltage and the local temperature alike. In fact, the amplification is observed in the experimental work in two harmonics $V_0^{(1)}$ and $V_0^{(2)}$ there analyzed, although it is stressed that the second one is a more reliable indication of the behavior of the heat propagation. In the integer quantum Hall effect, there is no fractionalization of the charge and the same electrons that transport the charge current also transport the energy along the edge. It is, thus, rather natural that the local voltage, which senses the electronic propagation, is correlated to the local temperature, which senses the energy propagation.

B. Quantum spin Hall systems

We now turn to analyze the case of a topological insulator, where there are a couple of edge states with electrons moving with different chiralities and spin polarizations. In this case, we have

$$\alpha(\omega) = \begin{cases} \gamma_+(\omega) + \gamma_-(1 + \bar{\Gamma}_{2,-}) & \text{if } x < x_1, \quad x \geq x_2, \\ \gamma_+(\omega)(1 + \bar{\Gamma}_{2,+}) + \gamma_-(\omega) & \text{if } x_1 \leq x < x_2. \end{cases}$$

with

$$\gamma_\sigma(\omega) = \frac{\pi \bar{\Gamma}_{1,\sigma}}{4\Lambda |\Delta_\sigma(\omega)|^2 \sin^2\left(\frac{\omega L}{2v_F} + \frac{\Phi}{2}\right)}. \quad (22)$$

Thus the sensed voltage and temperature will change along the edge, provided that the drain and/or source reservoirs are spin polarized, in which case $\bar{\Gamma}_{j,+} \neq \bar{\Gamma}_{j,-}$. For reservoirs without a net spin polarization, each branch of the edge contains an identical flow of electrons thermalized with the source reservoir propagating clockwise and electrons thermalized with the drain propagating with the opposite chirality. The result is a uniform voltage and temperature along the edge, while the voltage and temperature drop in relation to the voltages and temperature of the reservoirs takes place at the contacts.

VII. SUMMARY AND CONCLUSIONS

In this paper, we presented a simple model of a macroscopic droplet of a two-dimensional electron gas in the integer quantum Hall regime driven by an external ac source that acts as a heater. We used nonequilibrium methods to show that the heat current flows downstream (as expected) and derived expressions for the local voltage and temperature along the chiral edge of free fermions. Our results verify the arguments given by Granger and coworkers⁵ as an interpretation of their experiments. We found, also in agreement with these experiments, that the electrons along the edge thermalize with the closest ‘‘upstream’’ reservoir. We also found that the amplification factor of the upstream signals relative to the downstream ones are determined by the degree of coupling between the edge state and the drain reservoir.

Several comments are in order. In this model, the edge electrons are treated as free fermions, while a more realistic description of the edge states of the integer quantum Hall systems should include the effects of electron-electron interaction. Interaction effects should not change the results in an essential way since the edges are chiral and interactions only affect the forward propagation of the fermions and no backscattering processes can occur at the contacts. Thus, in the thermodynamic limit, the temperature along the edges should remain constant (with only oscillations due to finite-size effects such as the ones we find here). However, it is possible that Coulomb interactions may lead to oscillations along the edge that may not vanish in the thermodynamic limit (as in the case of a quantum wire studied by Schulz²¹).

It would be very interesting to have experiments of this type done in graphene devices since in graphene the integer quantum Hall effect is seen even at room temperature. Thus graphene could prove to be an ideal system for testing these type of questions. Experiments of this type could also be used to test the basic physics behind the quantum spin Hall effect. Indeed, if the reservoirs are not polarized, no chiral heat current would be observable. In contrast, chiral spin currents should be detectable if the reservoirs are polarized (magnetized).

While in this paper we have focused on the exactly solvable (and experimentally relevant) case of chiral heat transport in driven integer quantum Hall states, it is important to extend these results to the more nontrivial case of the edge states of the fractional quantum Hall fluids. It has long been known that fractional quantum Hall fluids also exhibit quantization of the thermal transport.²² In generic Abelian and non-Abelian fractional quantum Hall states, the edge states have both charged and neutral modes, which display distinct charge and thermal transport properties.^{3,22,23} It has long been predicted that the chiral heat transport in the fractional quantum Hall state at $\nu = 2/3$ has a thermal conductivity with opposite to the charge (Hall) conductivity in this state. This effect is due to the existence of counterpropagating neutral edge modes, and has recently been observed in experiments of noise in the current.²⁴ In the case of the intriguing non-Abelian quantum Hall state at $\nu = 5/2$ the neutral modes are predicted to be Majorana fermions, which have distinct heat transport signatures. More generally, the presence of neutral modes in fractional quantum Hall states is expected to lead to nontrivial thermoelectric

effects, with a net flow of charge without a net flow of heat (such as in the case of normal-superconductor junctions with Andreev reflection processes⁷). These important problems will be discussed in a future publication.

ACKNOWLEDGMENTS

We thank G. Lozano and C. Naón for discussions. We acknowledge support from CONICET, ANCyT, UBACYT (Argentina), and the J. S. Guggenheim Memorial Foundation (L.A.). L.A. thanks the ICMT of the University of Illinois for hospitality, and E.F. thanks Programa Raíces (MINCYT, Argentina) for support and the Department of Physics, FCEyN UBA (Argentina) for hospitality. This work was supported in part by the National Science Foundation, under grants DMR 0758462 and DMR-1064319 (EF).

APPENDIX: RETARDED UNPERTURBED GREEN FUNCTIONS

In this Appendix, we evaluate the equilibrium Green functions $G_{x,x',\sigma}^0(\omega)$, corresponding to the edge in contact to the source and drain reservoirs but free from the effect of the ac-driving voltage. This Green function can be evaluated from the solution of the following Dyson equation:

$$G_{x,x',\sigma}^0(\omega) = g_{x,x',\sigma}(\omega) + \sum_{j=1}^2 G_{x,x_j,\sigma}^0(\omega) \Sigma_{j,\sigma}(\omega) g_{x_j,x',\sigma}(\omega) \quad (\text{A1})$$

with

$$g_{x,x',\sigma}(\omega) = \frac{1}{\mathcal{N}} \sum_p \frac{1}{\omega - \sigma v_F (p - \frac{\Phi}{L})}, \quad (\text{A2})$$

the Green function of the free edge of chiral electrons, where $g_{x,x',+}(\omega) = g_{x',x,-}(\omega)$, with $p = 2n\pi/L$, $-K \leq n \leq K$, and $\mathcal{N} = 2K + 1$. In the limit $K \rightarrow \infty$, this function reads

$$g_{x,x',+}(\omega) = \frac{\pi e^{i\frac{\omega}{v_F}(x-x')}}{2\Lambda \sin(\frac{\omega L}{2v_F} + \frac{\Phi}{2})} \left[\Theta(x-x') e^{-i(\frac{\omega L}{2v_F} + \frac{\Phi}{2})} + \Theta(x'-x) e^{i(\frac{\omega L}{2v_F} + \frac{\Phi}{2})} \right], \quad (\text{A3})$$

where Λ is a high-energy cutoff.¹⁹ Assuming $x_1 < x_2$, the solution of Eq. (A1) is

$$G_{x,x_1,+}^0(\omega) = \begin{cases} \frac{\pi e^{i\frac{\omega}{v_F}(x-x_1)} e^{-i(\frac{\omega L}{2v_F} + \frac{\Phi}{2})}}{2\Lambda \sin(\frac{\omega L}{2v_F} + \frac{\Phi}{2})} \Delta_+(\omega) & \text{if } x < x_1, \quad x \geq x_2, \\ \frac{\pi e^{i\frac{\omega}{v_F}(x-x_1)} e^{i(\frac{\omega L}{2v_F} + \frac{\Phi}{2})}}{2\Lambda \sin(\frac{\omega L}{2v_F} + \frac{\Phi}{2})} \Delta_+(\omega) (1 + \bar{\Gamma}_{2,+}) & \text{if } x_1 \leq x < x_2. \end{cases}$$

and

$$G_{x,x_2,+}^0(\omega) = \begin{cases} \frac{\pi e^{i\frac{\omega}{v_F}(x-x_2)} e^{-i(\frac{\omega L}{2v_F} + \frac{\Phi}{2})}}{2\Lambda \sin(\frac{\omega L}{2v_F} + \frac{\Phi}{2})} \Delta_+(\omega) (1 + \bar{\Gamma}_{1,+}) & \text{if } x < x_1, \quad x \geq x_2, \\ \frac{\pi e^{i\frac{\omega}{v_F}(x-x_2)} e^{i(\frac{\omega L}{2v_F} + \frac{\Phi}{2})}}{2\Lambda \sin(\frac{\omega L}{2v_F} + \frac{\Phi}{2})} \Delta_+(\omega) & \text{if } x_1 \leq x < x_2. \end{cases}$$

where $G_{x,x',+}^0(\omega) = G_{x',x,-}^0(\omega)$, with $\bar{\Gamma}_{j,\sigma} = \pi \Gamma_{j,\sigma} / \Lambda$ and

$$\Delta_{\sigma}(\omega) = [1 - \Sigma_{1,\sigma} g_{x_1,x_1,\sigma}(\omega)][1 - \Sigma_{2,\sigma} g_{x_2,x_2,\sigma}(\omega)] - \Sigma_{1,\sigma} g_{x_1,x_2,\sigma}(\omega) \Sigma_{2,\sigma} g_{x_2,x_1,\sigma}(\omega). \quad (\text{A4})$$

¹B. I. Halperin, *Phys. Rev. B* **25**, 2185 (1982).

²X.-G. Wen, *Phys. Rev. Lett.* **64**, 2206 (1990).

³For reviews on edge states of quantum Hall systems, see X.-G. Wen, *Adv. Phys.* **44**, 405 (1995); A. M. Chang, *Rev. Mod. Phys.* **75**, 1449 (2003).

⁴For a review, see M. König, H. Buhmann, L. W. Molenkamp, T. L. Hughes, C.-X. Liu, X.-L. Qi, and S. C. Zhang, *J. Phys. Soc. Jpn.* **77**, 031007 (2008).

⁵G. Granger, J. P. Eisenstein, and J. L. Reno, *Phys. Rev. Lett.* **102**, 086803 (2009).

⁶L. Arrachea, M. Moskalets, and L. Martin-Moreno, *Phys. Rev. B* **75**, 245420 (2007); M. Rey, M. Strass, S. Kohler, P. Hänggi, and F. Sols, *ibid.* **76**, 085337 (2007); M. Moskalets and M. Büttiker, *ibid.* **80**, 081302 (2009).

⁷F. Giazotto, T. T. Heikkilä, A. Luukanen, A. M. Savin, and J. P. Pekola, *Rev. Mod. Phys.* **78**, 217 (2006); J. P. Pekola and F. W. J. Hekking, *Phys. Rev. Lett.* **98**, 210604 (2007).

⁸L. Arrachea and L. F. Cugliandolo, *Europhys. Lett.* **70**, 642 (2005).

⁹A. Caso, L. Arrachea, and G. S. Lozano, *Phys. Rev. B* **81**, 041301 (2010); **83**, 165419 (2011).

¹⁰C. W. Chang, D. Okawa, A. Majumdar, and A. Zettl, *Science* **314**, 1121 (2006); A. Dhar, *Adv. Phys.* **57**, 457 (2008); D. Segal, *Phys. Rev. Lett.* **101**, 260601 (2008); S. Lepri, R. Livi, and A. Politi, *ibid.* **78**, 1896 (1997); A. Dhar, *Adv. Phys.* **57**, 457 (2008); M. Terraneo, M. Peyrard, and G. Casati, *Phys. Rev. Lett.* **88**, 094302 (2002); Nianbei Li, Baowen Li, and Sergej Flach,

ibid. **105**, 054102 (2010); C. Chamon, E. Mucciolo, L. Arrachea, and R. Capaz, *ibid.* **106**, 135504 (2011).

¹¹T. Ojanen and A.-P. Jauho, *Phys. Rev. Lett.* **100**, 155902 (2008).

¹²Y. Zhang, Y.-W. Tan, H. L. Stormer, and P. Kim, *Nature (London)* **438**, 201 (2005).

¹³L. W. Molenkamp, H. van Houten, C. W. J. Beenakker, R. Eppenga and C. T. Foxon, *Phys. Rev. Lett.* **65**, 1052 (1990).

¹⁴H. L. Engquist and P. W. Anderson, *Phys. Rev. B* **24**, 1151 (1981).

¹⁵Y. Dubi and M. Di Ventra, *Nano Lett.* **9**, 97 (2009); *Rev. Mod. Phys.* **83**, 131 (2011).

¹⁶L. F. Cugliandolo and J. Kurchan, *Phys. Rev. Lett.* **71**, 173 (1993); *Philos. Mag. B* **71**, 50 (1995); L. F. Cugliandolo, *J. Phys. A: Math. Theor.* **44**, 483001 (2011) and references therein.

¹⁷F. Foieri and L. Arrachea, *Phys. Rev. B* **82**, 125434 (2010).

¹⁸L. Arrachea, *Phys. Rev. B* **72**, 125349 (2005); **75**, 035319 (2007); L. Arrachea and M. Moskalets, *ibid.* **74**, 245322 (2006).

¹⁹L. Arrachea, C. Naón, and Mariano Salvay, *Phys. Rev. B* **76**, 165401 (2007).

²⁰P. W. Brouwer, *Phys. Rev. B* **58**, R10135 (1998); M. Moskalets and M. Büttiker, *ibid.* **66**, 035306 (2002).

²¹H. J. Schulz, *Phys. Rev. Lett.* **71**, 1864 (1993).

²²C. L. Kane and M. P. A. Fisher, *Phys. Rev. B* **55**, 15832 (1997).

²³W. Bishara, G. A. Fiete, and C. Nayak, *Phys. Rev. B* **77**, 241306(R) (2008).

²⁴A. Beed, O. Nissim, H. Inoue, M. Heiblum, C. L. Kane, V. Umansky, and D. Mahalu, *Nature (London)* **466**, 585 (2010).